Role of His159 in Yeast Enolase Catalysis†

Dmitriy A. Vinarov‡ and Thomas Nowak*

Department of Chemistry and Biochemistry, University of Notre Dame, Notre Dame, Indiana 46556

Received April 1, 1999; Revised Manuscript Received July 8, 1999

ABSTRACT: There are presently several proposed catalytic mechanisms of yeast enolase, all of which have emerged from separate structural investigations of enolase from yeast and lobster muscle. However, the identities of the residues functioning as the general acid/base pair are not yet established unambiguously. In the Mn^{2+}−phosphoglycolate complex of lobster muscle enolase, the imidazole group of His157 (His159 in the yeast enolase numbering system) is in van der Waals contact (4.5 Å) with the C_2 of the inhibitor [Duquerroy et al. (1995) *Biochemistry 34*, 12513−12523]. To gain further information about the role played by His159 in the catalytic mechanism of yeast enolase this residue has been mutated to Ala. The gene encoding for the H159A mutation has been constructed and the mutant protein has been expressed in *Escherichia coli*. The purified mutant protein is folded properly as indicated by near- and far-UV circular dichroism and fluorescence data, and the mutation has no significant effect on the formation of ternary and quaternary enzyme−ligand complexes. In a typical assay, H159A showed 0.01% of wild-type specific activity, which corresponds to a reduction in k_{cat} of 4 orders of magnitude. The H159A fails to ionize the C-2 proton of either 2-PGA or phosphoglycolate. These findings are consistent with His159 serving as a potential catalytic base in the enolase reaction. We have suggested that His159 could also serve as a metal ligand at the third, inhibitory, metal binding site. This proposal is consistent with the catalytic mechanism of yeast enolase. Binding of metal ion at site III interferes with His159 reacting as the catalytic base, i.e., abstracting the C_2 proton from 2-PGA. Metal binding studies support the above proposal. Mn^{2+} binding at sites I and II for the His159Ala mutant is identical to that of wild type. The binding of Mn^{2+} at the third, inhibitory site of H159A is a factor of 3 weaker compared to wild-type enolase. The factor of 3 in binding is reasonable for the contribution to binding strength of a single nondominant ligand in a chelate [Klemba, M., and Regan, L. (1995) *Biochemistry 34*, 10094−10100. Regan, L. (1993) *Annu. Rev. Biophys. Biomol. Struct. 22*, 257−281. Cha et al. (1994) *J. Biol. Chem. 269*, 2687−2694].

There are presently several proposed catalytic mechanisms of enolase, all of which have emerged from separate structural investigations of enolase from yeast (*1*, *2*) and from lobster muscle (*3*). As part of the mechanistic process, the identities of residues functioning as the general acid/base pair are not yet unambiguously established.

The latest crystal structure of yeast enolase complexed with the equilibrium mixture of 2-PGA[1] and PEP at 1.8 Å resolution (*3*) and the kinetic analysis of several mutants (K345A, E168Q, E211Q) were interpreted by proposing that the catalytic base in enolase reaction is K345 (*4*). The E211 was assigned the role of proton donor to the leaving hydroxyl group in the forward reaction and the activator of the water molecule in the reverse reaction. One of the arguments in favor of E211−K345 being the catalytic acid−base pair is based on the results of Rose and co-workers (*5*), who determined that the enolase-catalyzed elimination of water from 2-PGA occurs with anti stereochemistry. Hence, any group(s) that assists in the leaving ability of the C-3 hydroxyl group in the dehydration reaction or in activation of water for attack in the reverse reaction should be found on the side of the substrate opposite to the catalytic base. K345 and E211 are located on the opposite sides of the substrate. The results of recent studies from our laboratory (*6*) argue against the proposal of Poyner et al. (*4*). The pH dependence of the kinetic parameters for yeast−Mg^{2+} enolase catalysis indicates that an unprotonated residue with the pK_A of about 5.9 and a protonated residue with a pK_A of about 8.5 are important for substrate binding and catalysis. A lysine base with a pK_A ∼ 6 and a glutamic acid with a pK_A ∼ 8.5 are not a likely base−acid pair.

In the Mn^{2+}−phosphoglycolate complex of lobster muscle enolase (*3*), the imidazole group of H157 (H159 in the yeast enolase numbering system) is in van der Waals contact (4.5 Å) with the C_2 of the inhibitor. This is the consequence of

† The research reported in this paper was supported by a research grant from the National Institute of Health (DK 17049) to T.N.

* To whom correspondence should be addressed. Telephone: (219) 631-5859. Fax: (219) 631-3567. E-mail: Nowak.1@nd.edu.

‡ Present address: Department of Biochemistry, Medical College of Wisconsin, Milwaukee, WI 53226.

[1] Abbreviations used in this paper: CD, circular dichroism; DNA, deoxyribonucleic acid; EPR, electron paramagnetic resonance; IPTG, isopropyl-β-thiogalactopyranoside; NMR, nuclear magnetic resonance; HEPES, *N*-(2-hydroxyethyl)piperazine-*N*′-2-ethanesulfonic acid; MES, 2-(*N*-morpholino)ethanesulfonic acid; PCR, polymerase chain reaction; PEP, phosphoenolpyruvate; 2-PGA, (D)-2-phosphoglycerate; P-glycolate, phosphoglycolate; PRR, water proton longitudinal relaxation rate; TRIS, 2-amino-2-(hydroxymethyl)-1,3-propanediol; TAPS, *N*-[tris(hydroxymethyl)methyl]-3-aminopropanesulfonic acid; SDS, sodium dodecyl sulfate.

10.1021/bi990760q CCC: $18.00
Published on Web 08/24/1999

a movement of loop L2 toward the inhibitor. In the apoenzyme, loop L2 is disordered, with no interpretable density for its side chains. The position of loop L2 in this particular ternary complex was also observed by Lebioda et al. (*7*) with the enolase−Mg^{2+}−phosphate−fluoride complex but not with substrate analogues. In the phosphonoacetohydroxamate−Mg^{2+} complex (*8*), the equivalent H159 is in contact with the inhibitor and interacts with the phosphonate. Thus, at least two X-ray structures of yeast enolase confirm that loop L2 can move to a position where the histidine is appropriately positioned at the active site.

Chemical modification studies by George and Borders (*9*) have shown that complete inactivation of enolase by diethyl pyrocarbonate correlates with the modification of six histidyl residues/subunit. Interestingly, the presence of substrate or substrate analogue 3-phosphoglycerate, plus excess Mg^{2+}, protects two histidyl residues per subunit from modification. Although there are several interpretations for such protection, the likelihood exists that two histidyl residues are present at the active site of enolase and may be involved in catalysis and/or in the binding of the third inhibitory Mg^{2+} to the enolase−PGA complex. In all of the available crystal structures of enolase, there are two histidine residues at the active site, H159 and H373. H159 is located 3.0 Å away from the C-2 proton of 2-PGA and could play a key role in the initial step of the reaction. H373 is positioned at the C-3 hydroxyl group of the substrate and could be involved in the departure of the leaving hydroxyl group.

Interpretation of the kinetic data together with analysis of available crystal structures led us to believe that H159 (yeast enolase numbering system) is a viable candidate for the catalytic base. The H159 is completely conserved in all known enolase species. A lysine with a pK_A shifted down by more then 4 pH units is a possible alternative to a histidine, but lysine does not often function as a base in enzymatic catalysis.

The purpose of this study is to construct, purify, and characterize the H159A and H159G enolase to gain further insight into the role played by histidine 159 in yeast enolase catalysis.

EXPERIMENTAL PROCEDURES

Materials for DNA Manipulations. Restriction enzymes (NdeI, BamHI, XbaI), pGEM-7Zf plasmid, and DH5α *Escherichia coli* strain were purchased from Promega. The PET-22b(+) vector and BL21(DE3pLysS) *E. coli* strain were purchased from Novagen. Pfu DNA polymerase was purchased from Stratogene Cloning. The fast-Link DNA ligation and screening kit was purchased from Epicenter Technologies. The QIAprep spin DNA miniprep kit and QIAEX II gel extraction kit were purchased from Qiagen. Bactotrypton, agar, and yeast extract were purchased from Fisher. Protein sequencing and synthesis of the oligonucleotides were done at the BioCore Facility, University of Notre Dame. DNA sequencing was done at the DNA Sequencing Facility, University of Iowa.

2-PGA and HEPES were purchased from Sigma. All other reagents were of the highest purity available.

Construction of the Enolase Expression Vector. The plasmid pEno46 (*10*), which contains a genomic clone of the yeast enolase gene, was a generous gift of Dr. Michael Holland, University of California−Davis. The coding region of the enolase gene was amplified using PCR with the following primers: (I) 5′-AAA **TCT AGA** *CAT ATG* GCT GTC TCT AAA GTT TAC GCT AGA-3′; (II) 5′-AAA *GGA TCC* TTA TAA TTT GTC ACC GTC GTG GAA GTT-3′. Primer I contains an XbaI restriction site (bold) and a NdeI site (italicized) 5′ to the start codon (ATG). Primer II has a BamHI site (italicized). The PCR was carried out for 35 cycles of 95 °C for 2 min, 58 °C for 1 min, and 72 °C for 5 min. The amplified product and the pGEM-7Zf plasmid were digested with the restriction endonucleases XbaI and BamHI and purified electrophoretically in a 0.8% agarose gel. The fragments were extracted from the gel using the QIAEX II gel extraction kit and ligated with Fast-Link DNA ligation and screening kit overnight at 16 °C. The product of the ligation was used to transform competent DH5α cells that were plated on LB-ampicillin plates. Colonies were picked and grown in LB medium. The plasmids were isolated from the resulting cultures and screened for the insertion of the enolase gene by digestion with XbaI and BamHI and subsequent agarose gel electrophoretic analysis. The enolase gene was excised from the pGEM−enolase construct with NdeI and BamHI and ligated into a similarly digested PET-22b plasmid. The entire coding region of the resulting construct, designated PET−enolase, was sequenced to verify the absence of spurious mutations and used to transform competent BL21(DE3pLysS) cells for expression.

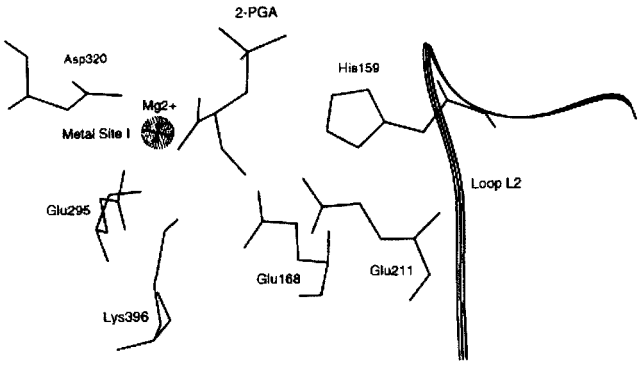

FIGURE 1: Active site structure of yeast enolase. This structure is taken from the crystal structure of yeast enolase complexed with an equilibrium mixture of 2-PGA and PEP at 1.8 Å by Larsen et al. (*2*). The backbone of loop L2 is shown as a triple stranded ribbon.

Selection of Mutations. The position of His159 with respect to the substrate, based on the crystal structure of Larsen et al. (*2*), is shown in Figure 1. His159 was mutated to an Ala in order to analyze the role of histidine residue at that position without introducing significant structural changes at the active site. His159 was also mutated to a Gly in order to simplify attempts at chemical rescue experiments with exogenous amines (*11*).

Site-Directed Mutagenesis. The following primers were synthesized for introducing the site-specific mutation: H159A, (a) 5′-GGT-GGT-TCC-*GCC*-GCT-GGT-GGT-3′, (b) 5′-ACC-ACC-AGC-*GGC*-GGA-ACC-ACC-3′; H159G, (a) 5′-GGT-GGT-TCC-*GGC*-GCT-GGT-GGT-3′, (b) 5′-ACC-ACC-AGC-*GCC*-GGA-ACC-ACC-3′. The italicized regions indicate the mutagenic codons. Mutagenesis was carried out by the following method: Pfu DNA polymerase, pGEM-enolase template, primers I and b or II and a were combined in a PCR reaction that yields a 477 or a 831 bp mutagenic

fragment of the enolase gene. A total of 35 cycles of 95 °C for 2 min, 55 °C for 1 min, and 72 °C for 3 min were carried out to synthesize the mutant DNA fragments. In the final PCR reaction a 477 and a 831 bp mutagenic fragment were combined with primers I and II and Pfu DNA polymerase to produce a full length mutant gene. The product was cloned into the pGEM-7Zf vector in the same way as the wild-type clone. The entire coding region of the mutant was sequenced to verify the absence of unwanted mutations. The mutant gene was cloned into the PET-22b(+) vector, expressed, and purified in the same manner as the wild-type enolase.

Expression and Purification of Wild-Type and Recombinant Enolase. Wild-type enolase was isolated from Baker's yeast using a revised procedure developed in our laboratory (*12*) that yields enzyme with a specific activity of 136 units/mg measured under standard conditions (see below). This enzyme shows a single band of protein, corresponding to a molecular weight of 46 500 Da on SDS−polyacrylamide gel electrophoresis and a single peak by capillary electrophoresis. Enolase was stored as a lyophilized powder at −20 °C.

Recombinant forms of enolase were obtained from large-scale fermentations in LB media. After the mutant plasmid has been established in BL21(DE3pLysS), expression of the target mutant DNA was induced by the addition of IPTG to a growing culture. A single colony from a freshly streaked plate was used to inoculate 50 mL LB containing the appropriate antibiotics in a 250 mL Erlenmeyer flask. Incubation was carried out at 37 °C until OD_{600} reached 0.6. IPTG was added to a final concentration of 1 mM and incubation was continued for 3 h. Cells were harvested by centrifugation and stored frozen at −70 °C. The *E. coli* cells were lysed by thawing since the BL21(DE3) strain contains pLysS. Recombinant enolase was purified by adaptation of the revised procedure developed in our laboratory (*12*). A typical 6 L growth under the conditions described above yielded about 15 g of wet cells from which approximately 60 mg of purified enolase or variant could be obtained.

Enolase Activity Assay. Solutions were prepared in distilled, deionized water. Enolase was prepared prior to experimentation by dissolving the dry powder in a minimal amount of 50 mM HEPES and passing the solutions through a G-25 column (1 × 14 cm) that contained 2 cm of Chelex-100 on the top. The column was equilibrated with 50 mM of HEPES. The enzyme was normally assayed by a modification of the assay previously described (*12*). The typical assay contained 50 mM HEPES, pH = 7.5, 50 mM KCl, 2 mM 2-PGA, and 1 mM $MgCl_2$ in a volume of 1 mL. Approximately 1 μg of wild type enolase was used in a typical assay. H159A and H159G enolase assays contained approximately 300 μg of protein. The increase in absorbance at 230 nm due to the formation of the product PEP was measured on either a Gilford 240 or 250 spectrophotometer. The enzyme concentrations were determined by using the extinction coefficient at 280 nm of 0.89 mL mg^{-1} cm^{-1} (*13*) and a molecular weight of 93 000 Da per dimer (*14*). The specific activity was initially determined as the change in absorbance at 230 nm/min divided by the enzyme concentration expressed as absorbance units at 280 nm (*15*). Data are reported as specific activity in standard activity units of micromoles of product per milliliter per minute per milligram of protein. A unit of activity at 230 nm [$(\Delta A_{230}/A_{280})$$min^{-1}$] corresponds to 0.32 units/mg.

Circular Dichroism Spectroscopy. CD spectra were measured in the UV region on a Cary model 60 recording spectropolarimeter that has been upgraded to a computer-assisted Aviv model 62DS. Measurements were made using a 0.2 cm path length cuvette. Each scan was recorded in 1 nm increments at 25 °C, repeated three times and averaged. The apo- wild-type enolase and mutant protein were prepared in 20 mM Hepes buffer, pH 7.5, containing 50 mM KCl, and their concentrations were adjusted to 0.25 μM prior to spectral acquisitions. The spectrum of the buffer was subtracted from all protein spectra, and the observed ellipticities, Θ, were normalized for protein concentration.

Fluorescence Spectroscopy. Fluorescence spectroscopy experiments were performed on a SLM-AMINCO 8100 spectrofluorometer. The excitation wavelength used was 287 nm, and the emission was scanned from 300 to 390 nm. Measurements were made using a 1 cm path length fluorescence cuvette. Samples of 5 μM wild-type enolase and mutant protein were in 50 mM Hepes buffer, pH 7.5 in the presence of 50 mM KCl.

Metal Binding Studies. The binding of Mn^{2+} to wild type and H159A enolase in the absence and presence of 2-PGA was determined by EPR spectroscopy on an X-band Varian E-9 EPR spectrometer. Enzyme solutions (50 μM sites) were prepared in 50 mM KCl and 50 mM Hepes buffer at pH 7.5. When appropriate, the samples also contained 2 mM PGA, a concentration found to be saturating for each of the experiments performed under experimental conditions. The concentration of Mn^{2+} was varied in each experiment, usually between 50 and 350 μM. Each sample was prepared in a 50-μL volume, and $[Mn^{2+}]_{free}$ was measured. The limit of detection for Mn^{2+}_{free} is approximately 1 μM. The binding data were calculated, plotted, and analyzed in a form of the Scatchard plot (*16*). In the case of Mn^{2+} binding to wild type and H159A enolase in the presence of 2-PGA, the binding data were analyzed for the number of independent binding sites (n) and for the dissociation constants (K_d) for each of the binding sites using the modified Winlund method (*17*).

$$\upsilon = \frac{n_1 K_{d1}[Mn^{2+}]_{free}}{K_{d1}(K_{d1} + [Mn^{2+}]_{free})} + \frac{n_2 K_{d2}[Mn^{2+}]_{free}}{K_{d2}(K_{d2} + [Mn^{2+}]_{free})} + \frac{n_3 K_{d3}[Mn^{2+}]_{free}}{K_{d3}(K_{d3} + [Mn^{2+}]_{free})} \quad (1)$$

This deconvolution of the experimental data uses a model with three binding sites. Specific details are given in the appropriate figure legends. A separate program, written to analyze binding data with multiple binding sites (M. Buening, Department of Chemistry and Biochemistry, University of Notre Dame), was also used to treat the data, and identical results were obtained.

Substrate and Ligand Binding by PRR Measurements. The binding of substrates and ligands was determined by measuring the solvent water proton longitudinal relaxation rates ($1/T_1$) using a Seimco pulsed NMR spectrometer operating at 24.3 MHz using the Carr-Purcell 180°−τ−90° pulse sequence (*18*). The paramagnetic effect on the relaxation rate ($1/T_{1p}$) is the difference in relaxation rates observed for a solution that contains the paramagnetic ion ($1/T_{1,\ obs}$)

and the relaxation rate of the identical solution in the absence of the paramagnetic species ($1/T_{1,0}$). The observed enhancement parameter (ϵ^*) is the ratio of $1/T_{1p}$ in the presence of the enzyme $(1/T_{1p})^*$ to $1/T_{1p}$ in the absence of the enzyme. The observed enhancement for enzyme and Mn^{2+} in the absence of added ligands (ϵ^*) will depend on the fraction of Mn^{2+} that is bound to the enzyme and the enhancement for the bound Mn^{2+}, ϵ_b. In the presence of ligand, a third enhancement term, ϵ_t (enhancement for bound Mn^{2+} in the ternary complex), must be considered:

$$\epsilon^* = \frac{[Mn^{2+}]_f}{[Mn^{2+}]_t}\epsilon_a + \frac{[E-Mn]}{[Mn^{2+}]_t}\epsilon_b + \frac{[E-Mn-L]}{[Mn^{2+}]_t}\epsilon_t \quad (2)$$

For the measurement of substrate and ligand binding by PRR, a sample of enzyme containing Mn^{2+} is titrated with a solution that contains an identical concentration of enzyme and Mn^{2+} and also includes the ligand. By titration of the second sample into the first, a PRR titration can be performed. This titration allows a variation in the concentration of the ligand without changing the concentration of the enzyme or Mn^{2+}. The $1/T_1$ of water is measured, and ϵ^* is plotted as a function of ligand concentration. The titration curves were fit to obtain the dissociation constants and ternary enhancement (ϵ_t) using the computer program PRRFIT2, written by R. Resiga (University of Notre Dame) in Fortran code.

Characterization of the H159A−Mn−PGA and H159A−Mn−PEP Complexes. The hydration number for the metal ion at site I was determined for the H159A enolase−Mn−PGA and H159A enolase−Mn−PEP complexes using PRR techniques. The procedure described by Hwang and Nowak (*19*) was followed. Longitudinal relaxation rates ($1/T_1$) of water protons (PRR) were measured. The experiments were performed under the conditions where only metal site I was occupied with Mn^{2+} and either 2-PGA or PEP was saturating. The paramagnetic contribution to the longitudinal relaxation rates ($1/T_{1p}$) of water was obtained by calculating the differences in relaxation rates between the Mn^{2+}-containing complex and the diamagnetic control where Mn^{2+} is absent.

The effects of frequency on $1/T_1$ for each complex were measured at 12.3, 24.3, 35.3, and 45.3 MHz. The frequency was adjusted with a frequency synthesizer, and resonance was obtained by varying the magnetic field. Normalized paramagnetic effects on the longitudinal relaxation rates $1/pT_{1p}$ for the binary complex and for the enzyme complexes are plotted as a function of the resonance frequency (ω_i). The effect of temperature on the $1/T_1$ of each complex was measured at 300 MHz on a Varian 300 NMR spectrometer equipped with a variable temperature probe. The temperature was varied between 5 and 40 °C.

To calculate the hydration number q for Mn^{2+} in the various enzyme complexes, the correlation time τ_c must be known. The τ_c for the electron−nucleus interaction was estimated for each of the complexes studied from the frequency dependence of the $1/pT_{1p}$ of water protons. The frequency-dependent data were fit based on the Bloembergen−Morgan theory (*20*−*22*) using eqs 3−6 and by using the computer program FREQ, written by Todd Holyoak and Michael Buening (University of Notre Dame) in Table Curve (Jandel Scientific) to simulate the data.

$$\frac{1}{pT_{1p}} = \frac{q}{T_{1M} + \tau_m} \quad (3)$$

$$\frac{1}{T_{1M}} = \frac{q(2S(S+1)\gamma^2 g^2 \beta^2)}{15r^6}\left[\frac{3\tau_c}{1+\omega_I{}^2\tau_c{}^2} + \frac{7\tau_c}{1+\omega_s{}^2\tau_c{}^2}\right] \quad (4)$$

$$\frac{1}{\tau_c} = \frac{1}{\tau_r} + \frac{1}{\tau_s} + \frac{1}{\tau_m} \quad (5)$$

$$\frac{1}{\tau_S} = B\left[\frac{\tau_v}{1+\omega_s{}^2\tau_v{}^2} + \frac{4\tau_v}{1+4\omega_s{}^2\tau_v{}^2}\right] \quad (6)$$

The normalized relaxation rate ($1/pT_{1p}$) is directly proportional to the hydration number, q, and related to the relaxation time (T_{1M}) and residence time of the water (τ_m) (eq 3) (*23*). The relaxation rate of the bound nuclei ($1/T_{1M}$) is described by the simplified form of the Solomon−Bloembergen equation (eq 4) (*21, 22*), where S is the electron-spin quantum number, γ is the nuclear magnetogyric ratio, r is the ion−nuclear distance, g is the electronic "g" factor, β is the Bohr magneton, and ω_I and ω_s are the Larmor angular precession frequencies for the nuclear and electron spins, respectively, where $\omega_s = 657\omega_i$. The correlation time, τ_c, for the electron−nuclear interaction is related to the rotational correlation time, τ_r, the residence time of water protons, τ_m, and the electron relaxation time, τ_s (eq 5). The electron relaxation time is frequency dependent, eq 6, where B is an anisotropy factor and τ_v is the correlation time for electron distortion at Mn^{2+}. For these calculations, the rotational correlation time, τ_r, is approximated as the molecular mass of the species (93 000 Da) divided by 2000 (*24*). Details of this approach have been reviewed elsewhere (*19*). The program is designed using a least-squares method of solving all four equations simultaneously using an iterative fit. The program relates the normalized value of $1/pT_{1p}$ to the water proton relaxation rate and to the water exchange rate. The values for the hydration number, q, and the correlation time, τ_c, are determined from the simultaneous fit of the data to eqs 3−6.

The correlation times (τ_c) for both complexes were also determined from the values of $1/T_{1M}$ at two frequencies (eq 9) and from the ratio of $1/T_{1M}$ and $1/T_{2M}$ determined at a single frequency (eq 10). These measurements were made at 300 and 500 MHz using Varian VXR300 and Varian VXR500 Unity Plus NMR spectrometers. The paramagnetic

$$\frac{1}{T_{2M}} = \frac{q(S(S+1)\gamma^2 g^2 \beta^2)}{15r^6}\left[4\tau_c + \frac{3\tau_c}{1+\omega_I{}^2\tau_c{}^2} + \frac{13\tau_c}{1+\omega_s{}^2\tau_c{}^2}\right] \quad (7)$$

$$\frac{1}{T_{1,2M}} = \frac{1}{P_M q T_{1,2}} \quad (8)$$

$$\tau_c = \left[\frac{T_{1M(2)} - T_{1M(1)}}{T_{1M(1)}\omega_{I(2)}{}^2 - T_{1M(2)}\omega_{I(1)}{}^2}\right]^{1/2} \quad (9)$$

$$\tau_c = \left[\frac{6\frac{T_{1M}}{T_{2M}} - 7}{4\omega_I{}^2}\right]^{1/2} \quad (10)$$

contribution to the relaxation rates ($1/T_{1M}$ and $1/T_{2M}$) under fast exchange conditions are normalized using eqs 7 and 8. P_M is the mole fraction of ligand bound, and q is the number of ligands bound. Equation 9 is used to calculate τ_c from T_{1M} values at two frequencies, $T_{1M(1)}$ and $T_{1M(2)}$ and assumes that τ_c is frequency independent in this frequency range. Equation 10 is used to calculate τ_c from T_{1M} and T_{2M} values at a single frequency and makes the assumption that only dipolar contributions affect $1/T_{1M}$ and $1/T_{2M}$.

^{1}H/^{2}H Exchange at C-2 of 2-PGA and Phosphoglycolate. H159A enolase was tested for the ability to catalyze the exchange of the C-2 proton of 2-PGA and of the substrate analog phosphoglycolate by ^{1}H NMR spectroscopy in D_2O. For the exchange of the C-2 proton of 2-PGA, samples contained 20 mM 2-PGA, 25 μM enzyme, and 25 mM Tris buffer in D_2O, pD 7.5, in the presence of 50 mM KCl. A reference spectrum was recorded, and the reaction was initiated by addition of 1 mM Mg^{2+}. The reaction containing wild-type enolase was quenched after 10 min by addition of 2.5 mM EDTA, and the spectrum was recorded. The reaction with H159A enolase was incubated for 3 h at room temperature before quenching with 2.5 mM EDTA and acquiring the ^{1}H spectrum. For the exchange of the C-2 proton of phosphoglycolate, samples contained 20 mM phosphoglycolate, 25 μM enzyme, and 25 mM Tris buffer in D_2O, pD 7.5, in the presence of 50 mM KCl. A reference spectrum was recorded, and the reaction was initiated by addition of 1 mM Mg^{2+}. For the wild-type reaction, spectra were recorded at suitable time intervals until the signal of the C-2 proton of phosphoglycolate had decreased by 50%. In the case of H159A enolase, spectra were also recorded at suitable time intervals. The reaction was allowed to proceed for 4 h. All spectra were obtained as the average of 128 scans on a Varian VXR500 Unity Plus NMR spectrometer. The amounts of [2-^{1}H]-2-PGA or [2-^{1}H]-phosphoglycolate remaining in the sample were calculated on the basis of the relative peak heights of the signals of [2-^{1}H]-2-PGA or [2-^{1}H]-phosphoglycolate and [2-^{2}H]-2-PGA or [2-^{2}H]-phosphoglycolate.

Chemical Rescue Experiments. Imidazole and ammonia were tested for the ability to stimulate the catalytic activity of H159A and H159G enolase. The imidazole has a molecular volume of 64.9 Å^3 and a pK of 7.0. Ammonia has a molecular volume of 25.4 Å^3 and a pK of 9.2 (*11*). Assays were performed (I) in the presence of 50 mM imidazole buffer at pH 7.5 with the concentration of Mg^{2+} varied between 1 and 20 mM and (II) in the presence of CAPS buffer at pH 9.5 and 50 mM NH_4Cl, pH 9.5. Other conditions were the same as described above for the enzyme assay.

^{1}H/^{2}H exchange at the C-2 of 2-PGA and phosphoglycolate (see above) were repeated in the presence of rescue agents. This technique is an assay for the first step of the reaction, proton abstraction, with greater sensitivity.

RESULTS

Protein Expression and Purification. The wild-type, H159A, and H159G enolase plasmids were constructed and identified by restriction digest. The entire enolase gene was sequenced to confirm the absence of any spurious mutations in the coding region outside the area of the mutation. Expression of the wild type, H159A, and H159G enolase in the BL21(DE3pLysS) *E. coli* strain after the induction with IPTG resulted in approximately 15 g of wet cells from fermentation in 6 L of LB medium. Purification of the wild type, H159A, and H159G enolase with the procedure developed in our laboratory (*12*) yielded about 60 mg of each protein from 15 g of cells, respectively. The purified wild type, H159A, and H159G enolase each appear as a single band on SDS−PAGE corresponding to a molecular weight of 46 500 Da. The migration is the same as that obtained with wild-type enolase. The N-terminus of the H159A enolase mutant enolase was sequenced to establish that the purified protein is indeed yeast enolase. The N-terminal sequence A-V-S-K-V was obtained and corresponds to the N-terminus of yeast enolase. *E. coli* enolase has N-terminal sequence of S-K-I-V-K-I.

Activity Assays. Both native and recombinant wild-type enolase have the same kinetic parameters. No activity was detected in the routine assay with H159A or with H159G enolase even with the addition of 10−20 times as much protein as used in the wild-type assay and by following the reaction for 10 min. The H159A and H159G enolase have less than 0.01% (10^{-4}) enzyme activity relative to the wild-type enolase. Using even larger amounts of H159A and H159G enolase (300 μg in 1 mL assay) and following the reaction for longer times, very low levels of activity were detected. This activity was no more than 0.01% of the activity of wild-type enolase. This represents a lower limit of detection. The H159G enolase was not further characterized. The pH of the assay and the activating metal ion were varied. The H159A enolase showed the same basal levels of activity (<0.01% compared to the wild-type enolase) in the pH range from 5.4 to 10.0 and upon substitution of Mn^{2+} and of Co^{2+} for Mg^{2+}. Such activity corresponds to a reduction in k_{cat} of at least 4 orders of magnitude compared to wild type enolase. The severely depressed activity of the mutant proteins indicates that the mutated residue, His159, is essential for catalysis. Activity in the overall reaction provides little insight into the specific role played by His159.

Evaluation of the Secondary Structure of H159A Enolase by Circular Dichroism. To examine if the mutation had disrupted the overall enzyme structure, circular dichroism spectroscopy was performed. The spectrum of the wild type enolase exhibits a double minima at 210 and 223 nm, characteristic of α-helical content. The CD spectrum of the H159A enolase mutant is virtually indistinguishable from that of wild-type enolase (Figure 2). This demonstrates that the mutated site did not result in the alteration of overall secondary structure of enolase.

Evaluation of the Tertiary Structure of H159A Enolase by Fluorescence and Far-UV Circular Dichroism. To examine the possibility that H159A mutation had resulted in disruption of the local environment around the tryptophan residues in the enzyme, the intrinsic fluorescence spectra of wild type and mutant enolase were obtained (Figure 3). The tryptophan emission exhibits a maximum at 341 nm in spectra of wild-type enolase and H159A mutant enolase. The maximal intensities, as normalized for 280 nm absorbance differ by less than 5%. The two spectra are identical, indicating that the protein regions surrounding the tryptophan residues have not sustained major changes as a result of the mutation. The CD spectrum from 260 to 340 nm of H159A

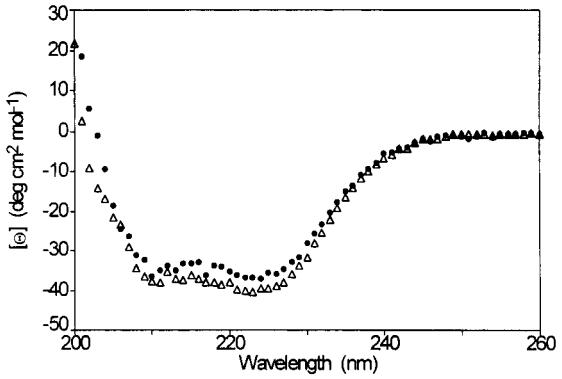

FIGURE 2: Far-UV CD spectra of apo-wild-type and H159A enolase. The apo-wild-type enolase (△) and H159A enolase (●) were prepared in 20 mM Hepes buffer, pH 7.5, containing 100 mM KCl, and their concentrations were adjusted to 0.25 μM prior to spectral acquisitions. Each scan was recorded in 1 nm increments at 25 °C, repeated three times, and averaged. The spectrum of the buffer was subtracted from all protein spectra.

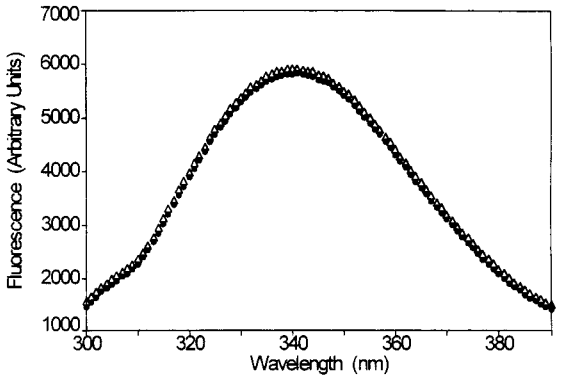

FIGURE 3: Fluorescence emission spectra of apo-wild-type and H159A enolase. Samples of 5 μM wild-type enolase (△) and H159A enolase (●) were in 50 mM Hepes buffer, pH 7.5, in the presence of 100 mM KCl. The excitation wavelength used was 287 nm, and the emission was scanned from 300 to 390 nm.

could be superimposed on the spectrum of the wild-type enzyme and shows an overall conservation of the tertiary fold (data not shown).

Mn^{2+} Binding. The binding of Mn^{2+} to wild type and H159A enolase was measured by EPR spectroscopy. In the absence of 2-PGA, at neutral pH, a single Mn^{2+} binding site per monomer for both proteins was detected. The dissociation constants for Mn^{2+} binding at site I appear to be very similar for both proteins ($K_{d,Mn^{2+}} = 5.82 \pm 0.51$ μM for the wild type; $K_{d,Mn^{2+}} = 7.31 \pm 0.40$ μM for the H159A enolase), indicating that the mutation had no effect on the binding of the metal ion at site I. The enolase−Mn^{2+} complex exhibits a binary enhancement of 13−15 (*25*, *26*). The binary enhancement for H159A in the presence of Mn^{2+} is 10. At pH 7.5, in the presence of 2 mM PGA, six Mn^{2+} binding sites per dimer for each protein were detected (Figure 4). The data were fit to a model of three independent binding sites per dimer to determine the binding constants for Mn^{2+} at sites I, II, and III. The results of the fits are summarized in Table 1. Errors in these fits are difficult to assess, but the errors in the calculations of the three K_d values are reflected in greater deviations for K_{d3} than for K_{d1}. This is due, in part, to the larger errors inherent in the determination of weaker binding cations, in the observations of smaller changes at higher Mn^{2+} concentrations, and in performing

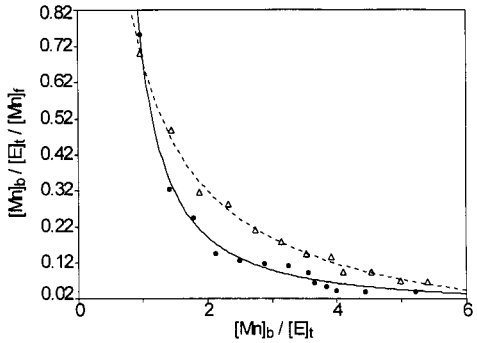

FIGURE 4: Mn^{2+} binding to wild type and H159A enolase in the presence of 2-PGA. The binding of Mn^{2+} to 50 μM enzyme sites was measured at pH 7.5 in the presence of 50 mM HEPES containing 50 mM KCl and 2 mM 2-PGA, and the results are presented as a Scatchard plot. The levels of free Mn^{2+} were measured by EPR spectroscopy for wild type (△) and H159A (●) enolase. The curves drawn were obtained by best fits to Mn^{2+} binding to the enolase dimer, assuming three independent binding sites per monomer. The parameters for the best fits are presented in Table 1.

Table 1: Dissociation Constants for Mn^{2+} Binding to Wild-Type and H159A Enolase in the Presence of Saturating (2 mM) 2-PGA

enzyme	K_{d1} (μM)	K_{d2} (μM)	K_{d3} (μM)
WT enolase	2.2 ± 0.2	27.3 ± 3.1	45.5 ± 10.2
H159A enolase	1.6 ± 0.4	23.3 ± 5.2	156.3 ± 25.5

Table 2: Dissociation Constants of the Ligands from the Ternary and Quaternary Enolase Complexes

	enolase−Mn^{2+} [a]		H159A−Mn^{2+} [a]	
ligand	K_3	ϵ_t	K_3	ϵ_t
2-PGA	22.6 ± 0.1 μM	8.5	14.4 ± 0.3 μM	8.3
PEP			28.6 ± 0.2 μM	8.1
P-glycolate	46.1 ± 2.1 μM	7.3	52.6 ± 2.3 μM	7.1
F^-	213.4 ± 2.5 mM	7.0	382.2 ± 3.9 mM	6.9
F^- [b]	1.5 ± 0.1 mM	6.5	1.5 ± 0.1 mM	7.1
P_i	187 ± 6 μM	6.4	188 ± 6 μM	6.5
P_i [c]	2.88 ± 0.5 μM	7.0	3.01 ± 0.6 μM	6.5

[a] K_3 and ϵ_t were obtained by best fits to PRR titration data from Figures 5, 6, and 7 using the program PRRFit as described. [b] F^- titration was performed in the presence of 1 mM P_i. [c] P_i titration was performed in the presence of 100 mM F^-.

multiparameter fits. The binding data for H159A enolase indicate that Mn^{2+} binding at sites I and II were unaffected by the mutation. In contrast, Mn^{2+} affinity for the third site in the H159A enolase was reduced by a factor of 3 (Figure 4; Table 1). Such behavior could be explained by the loss of a nondominant ligand at site III in the H159A mutant enolase. This interpretation is consistent with the conclusions from the pH studies on yeast enolase (*6*). On the basis of the results of those studies and the results presented here, His159 is implicated as a potential ligand to the third, inhibitory, metal binding site.

Substrate and Ligand Binding to the Enolase−Mn Complex by PRR Measurements. PRR titrations were used to investigate the interaction of 2-PGA with wild-type enolase−Mn^{2+} and of 2-PGA and PEP with H159A enolase−Mn^{2+}. Titration of 2-PGA into the enolase−Mn^{2+} and H159A−Mn^{2+} complexes decreases the enhancement value to yield a ternary enhancement (ϵ_t) of approximately 8.5 for both complexes (Figure 5A). An optimal fit to the data in Figure 5A is obtained by using the iterative program PRRFit. The

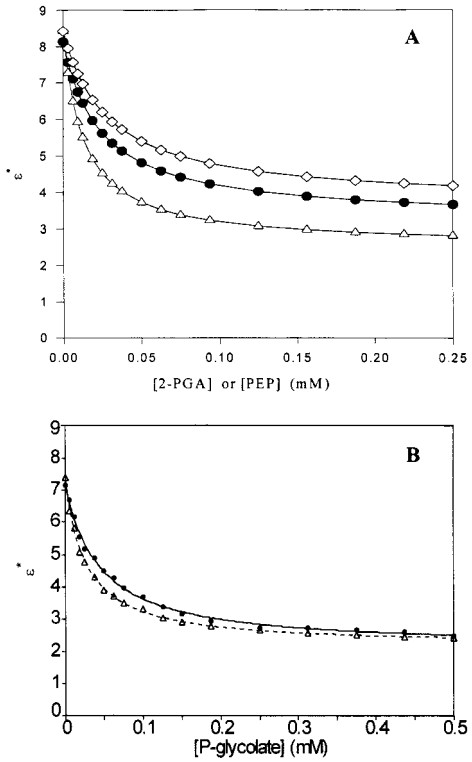

FIGURE 5: PRR titrations of 2-PGA, PEP, and P-glycolate to wild-type enolase−Mn^{2+} and H159A enolase−Mn^{2+}. (A) Titrations of 2-PGA or PEP into the enzyme−Mn complexes were performed in the presence of 50 mM Hepes, pH 7.5, 50 mM KCl, 100 μM enzyme sites, and 80 μM Mn^{2+}. Identical solutions that contained the ligand were titrated into the enolase−Mn complex. The experiments included titrations of wild-type enolase with 2-PGA (●), H159A with 2-PGA (△), and H159A with PEP (◇). The curves result from best fits to the data with optimal values for K_3 and ϵ_t. (B) Titrations of P-glycolate into the enzyme−Mn complexes were performed as described in (A). The experiments included titrations of wild-type enolase (△) and H159A (●) with P-glycolate. The curves result from best fits to the data with optimal values for K_3 and ϵ_t. The relevant parameters giving the best fit are summarized in Table 2.

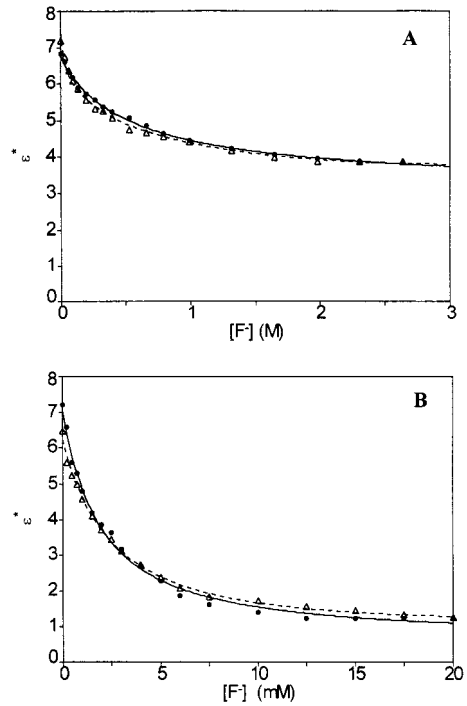

FIGURE 6: Binding of F^- to wild type and H159A enolase−Mn^{2+} complexes in the absence and presence of P_i. (A) Titrations of F^- into the enzyme−Mn complexes were performed in the presence of 50 mM Hepes, pH 7.5, 50 mM KCl, 100 μM enzyme sites, and 80 μM Mn^{2+}. Identical solutions that contained the ligand were titrated into the appropriate enolase−Mn complex. The experiments included titrations of wild-type enolase (△) and H159A (●) with F^-. The curves result from best fits to the data with optimal values for K_3 and ϵ_t. (B) Titrations of F^- into the enzyme−Mn complexes were performed as described in (A) but in the presence of 1 mM of P_i. The experiments included titrations of wild-type enolase (△) and H159A (●) with F^-. The curves result from best fits to the data with optimal values for K_3 and ϵ_t. The relevant parameters giving the best fit are summarized in Table 2.

K_3 value, the dissociation constant for the ligand from the E−Mn−ligand complex, for 2-PGA binding to enolase−Mn^{2+} is 22.6 ± 0.1 μM with a ϵ_t value of 8.5. The K_3 value for 2-PGA to H159A−Mn^{2+} is 14.4 ± 0.3 μM with ϵ_t = 8.3. PEP binding to H159A−Mn^{2+} occurs with a K_3 of 28.6 ± 0.2 μM and ϵ_t = 8.1.

The interaction of P-glycolate, a substrate analogue and competitive inhibitor with respect to 2-PGA, with enolase−Mn^{2+} and with H159A enolase−Mn^{2+} complexes was investigated by PRR techniques. Titration of P-glycolate into the enolase−Mn^{2+} and H159A enolase−Mn^{2+} complexes decreases the enhancement value to yield a ternary enhancement (ϵ_t) of approximately 8 for both enzyme−Mn^{2+} complexes. An optimal fit to the data in Figure 5B is obtained when K_3 is assumed to be 46.1 ± 2.1 and 52.6 ± 2.2 μM for the formation of the wild type and H159A enolase−Mn^{2+}−P-glycolate complexes respectively (Table 2).

The interaction of F^- with wild-type enolase−Mn^{2+} and H159A enolase−Mn^{2+} complexes was investigated by PRR techniques. Titration of F^- into the enolase−Mn^{2+} and H159A enolase−Mn^{2+} complexes decreases the enhancement value to yield a ternary enhancement (ϵ_t) of 7.2 and 6.8, respectively (Figure 6A). An optimal fit to the data is obtainedwhen K_3 is assumed to be 213 and 382 mM for the formation of ternary complexes of wild type and H159A enolase, respectively. These dissociation constants are in agreement with the weak binding and inhibition of Mn^{2+}-activated enolase by F^- in the absence of P_i (*27*).

The effect of P_i on the PRR of wild-type enolase−Mn^{2+} and H159A enolase−Mn^{2+} complexes was also studied. The addition of P_i decreased the enhancement for the wild-type enolase−Mn^{2+}−P_i complex to about 7.6 and for the H159A enolase−Mn^{2+}−P_i to about 6.5 (Figure 7A). The K_d for P_i binding to the wild type and H159A enolase was determined to be 187 and 188 μM, respectively.

The formation of the quaternary wild type and H159A enolase−Mn^{2+}−F−P_i complexes was studied by PRR titrations. The PRR titrations demonstrate that the presence of either one of the ligands, F^- or P_i, greatly increased the affinity of the second ligand for the enzyme−Mn^{2+} ternary complex. This binding synergy is similar to that previously reported (*28*). These titrations result in the formation of the tightly bound E−Mn^{2+}−P_i−F^- quaternary complex. As little as 1 mM P_i decreases the apparent K_d of F^- to the enolase−Mn^{2+}−P_i complex and the H159A enolase−Mn^{2+}−P_i complex by about 2 orders of magnitude. Figure 6B shows the results of a PRR titration of F^- into the enolase−Mn^{2+} and H159A enolase−Mn^{2+} complexes in the presence of 1 mM P_i. The final enhancement values observed from these

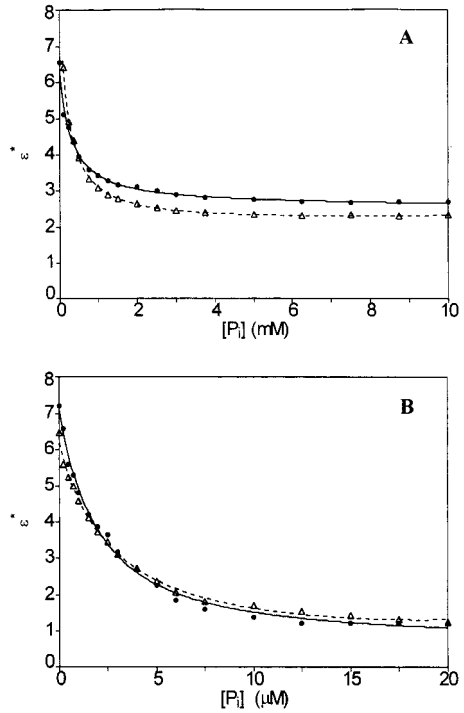

FIGURE 7: Binding of P_i to wild type and H159A enolase−Mn^{2+} complexes in the absence and presence of F^-. (A) Titrations of P_i into the enzyme−Mn complexes were performed in the presence of 50 mM Hepes, pH 7.5, 50 mM KCl, 100 μM enzyme sites, and 80 μM Mn^{2+}. Identical solutions that contained the ligand were titrated into the enolase−Mn complex. The experiments included titrations of wild-type enolase (△) and H159A (●) with P_i. The curves result from best fits to the data with optimal values for K_3 and ϵ_t. (B) Titrations of P_i into the enzyme−Mn complexes were performed as described in (A) but in the presence of 100 mM F^-. The experiments included titrations of wild-type enolase (△) and H159A (●) with P_i. The curves result from best fits to the data with optimal values for K_3 and ϵ_t. The relevant parameters giving the best fit are summarized in Table 2.

titrations are approximately 1 for both wild type and H159A enolase complexes. These low enhancement values could be explained by the absence of the freely accessible solvent water interacting with the Mn^{2+} in the quaternary E−Mn^{2+}−F^-−P_i complexes. The analysis of the binding data yields the K_d values for F^- binding of 1.51 and 1.54 mM for the wild type and H159A enolase, respectively.

The apparent K_d of P_i also decreases dramatically in the presence of F^- (Figure 7B). In these titrations, the final enhancement values are also approximately 1 for both wild type and H159A enolase complexes when P_i is titrated into the solution of the enzyme and Mn^{2+} containing 100 mM F^-. The apparent dissociation constant for P_i to the wild-type enolase−Mn^{2+}−F^-−P_i complex is 2.81 μM and is 3.01 μM from the H159A enolase−Mn^{2+}−F^-−P_i complex.

The results of the PRR titrations indicate that the substitution of Ala for His at the active site of yeast enolase does not appear to affect the binding of substrate (2-PGA/PEP), substrate analogue P-glycolate, or inhibitory ligands (F^- and/or P_i) to the enzyme−Mn^{2+} complex. The mutation has no significant effect on the formation of either ternary or quaternary complexes nor on the synergistic ligand effects observed with F^- and P_i (Figures 5−7; Table 2). The results of the PRR titrations for the wild-type enolase presented here are similar to those obtained by Maurer and Nowak (*28*).

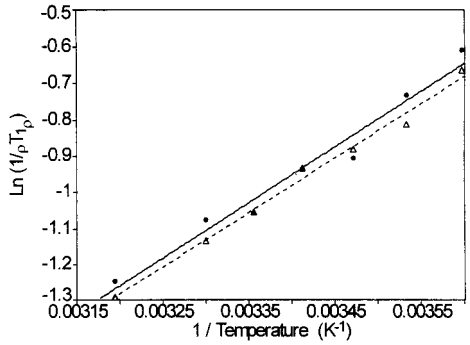

FIGURE 8: Temperature dependence of $1/pT_{1p}$ values for water protons at the metal site I in the H159A−Mn−PGA and H159A−Mn−PEP complexes. Normalized paramagnetic effects of $1/T_1$ values of water protons were measured as a function of temperature for the H159A−Mn−PGA (●) and H159A−Mn−PEP (△) complexes. The experiments were performed at 100 μM enolase sites, 50 μM Mn^{2+}, and 1 mM of either PEP or 2-PGA in 50 mM TRIS buffer, pH 7.5, and 50 mM KCl. Measurements were made at 300 MHz at 5, 10, 15, 20, 25, 30, and 40 °C. The lines are the least-squares fit to the data.

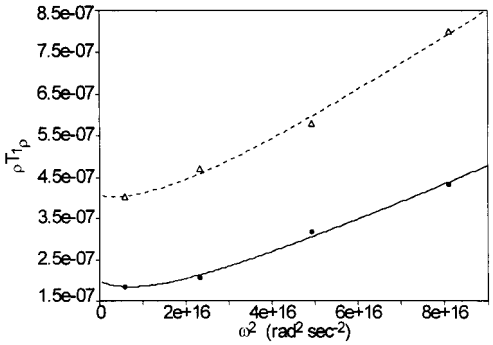

FIGURE 9: Frequency dependence of PRR for the H159A−Mn−PGA and H159A−Mn−PEP complexes. The pT_{1p} values were calculated for bound Mn^{2+} for the H159A−Mn−PGA (△) and H159A-Mn−PEP (●) complexes, respectively. The curves represent the best fits to the experimental data, and the relevant parameters from this fit are summarized in Table 3.

Characterization of the H159A−Mn−PGA and H159A−Mn−PEP Complexes. Since H159A is catalytically inactive, the enzyme−Mn−PGA and the enzyme−Mn−PEP complexes can be independently characterized. These complexes cannot be studied with wild-type enolase because of catalytic interconversion. The formation of enzyme−Mn−ligand complexes appears to be identical for wild type and H159A (vide supra).

The $1/pT_{1p}$ relaxation rates of water protons in the H159A−Mn−PGA and H159A−Mn−PEP complexes were determined as a function of temperature over the range of 5−40 °C at 300 MHz. The results are plotted in Figure 8. The plots are linear with a positive slope, indicative of fast chemical exchange. The activation energies, E_a, were calculated from the slope of the line. The E_a for the H159A−Mn−PGA complex is −6.05 ± 0.05 kcal/mol, and the E_a for the H159A−Mn−PEP complex is −6.17 ± 0.05 kcal/mol.

The hydration number for the metal ion at site I was determined in the H159A enolase−Mn−PGA and H159A enolase−Mn−PEP complexes. PRR measurements were made at 12.3, 24.3, 35.3, and 45.3 MHz. Figure 9 shows the frequency dependence of pT_{1p} values for the H159A−Mn−PGA and H159A−Mn−PEP complexes. The frequency

Table 3: Relaxation Parameters Calculated from pT_{1p} vs ω_i^2 [a]

complex	$10^{-6}pT_{1p}$ [b] (s^{-1})	τ_c (ns)	τ_v (ps)	$10^{18}B$	q
H159A−Mn−PGA	4.7	2.83[c]	5.17	4.8	0.47
H159A−Mn−PEP	2.1	3.86[c]	6.95	4.8	0.96

[a] PRR measurements using H159A−Mn−PGA and H159A−Mn−PEP complexes were taken from the data presented in Figure 9. The results were fit as described using the parameters listed. [b] The pT_{1p} values were taken at 24.3. [c] The τ_c values were estimated for the complexes studied by utilizing the frequency dependence of the $1/pT_{1p}$ of water protons and calculated at 24.3 MHz.

dependent relaxation data were fit by utilizing a program to simulate the data by assuming rapid exchange and utilizing the Bloembergen−Morgan theory. The relationship is linear from 45.3 to 24.3 MHz for both complexes with curvature below 24.3 MHz. The key parameters resulting in the best fit are summarized in Table 3. These values were obtained, assuming the metal-to-water proton distance is 2.87 Å. In this multiparameter fit there is little significant difference in values for τ_c and B between the two complexes. The hydration number for H159A enolase−Mn−PGA complex is 0.47, and the value increases to 0.96 for the H159A enolase−Mn−PEP complex. The nonintegral value calculated for q in the H159A enolase−Mn−PGA complex may be due to either the metal-bound water having only one proton in fast exchange or to collective uncertainties in the data fitting.

Two additional independent methods were used to determine τ_c for the Mn−H_2O interactions in the H159A enolase−Mn−PGA and H159A enolase−Mn−PEP complexes. The ^1H relaxation rates of water protons were measured at 300 and 500 MHz. This approach has been outlined by Navon and shown to give reliable results for such studies (*29*). The normalized values for $1/pT_{1\rho} = 2.33 \times 10^6$ at 300 MHz and $1/pT_{1\rho} = 2.09 \times 10^6$ at 500 MHz were calculated for the H159A enolase−Mn−PGA complex and normalized values for $1/pT_{1\rho} = 1.66 \times 10^6$ at 300 MHz and $1/pT_{1\rho} = 1.15 \times 10^6$ at 500 MHz were calculated for the H159A enolase−Mn−PEP complex from the relaxation data at both magnetic fields. Assuming fast exchange for the water protons and frequency independence for τ_c at higher magnetic fields, τ_c can be calculated from eq 9 and gives a value of 0.87×10^{-9} and 1.91×10^{-9} s for the complexes containing 2-PGA and PEP, respectively. Alternatively, values for $1/pT_{1\rho}$ and $1/pT_{2\rho}$ for water protons were measured at 300 MHz. The $1/T_2$ values were measured directly by the Carr−Purcell−Meiboom−Gill method (*30*). The normalized values of $1/pT_{1\rho} = 2.23 \times 10^6$ and $1/pT_{2\rho} = 2.97 \times 10^6$ were calculated for the H159A enolase−Mn−PGA complex and normalized values for $1/pT_{1\rho} = 1.52 \times 10^6$ and $1/pT_{2\rho} = 2.32 \times 10^6$ were calculated for the H159A enolase−Mn−PEP complex. Assuming the protons are in fast exchange and the effects on relaxation are purely dipolar in nature, τ_c values are calculated from eq 10. The τ_c value for the H159A enolase−Mn−PGA complex is 1.66×10^{-9} and 2.47×10^{-9} for the H159A enolase−Mn−PEP complex. These values are similar to those estimated by frequency dependence of the PRR effects and support the basis of the calculations for the hydration numbers for both complexes.

The increase in hydration number, q, for the H159A−Mn−PEP complex relative to that of H159A−Mn−PGA complex indicates that the C-3 hydroxyl group of the enzyme-bound 2-PGA replaces the water molecule in the coordination sphere of the metal ion at site I that is present with PEP as the ligand. This complements the results of Nowak et al. (*26*) and agrees with the crystal structure of the Mn^{2+}−phosphoglycolate complex of lobster muscle enolase (*3*).

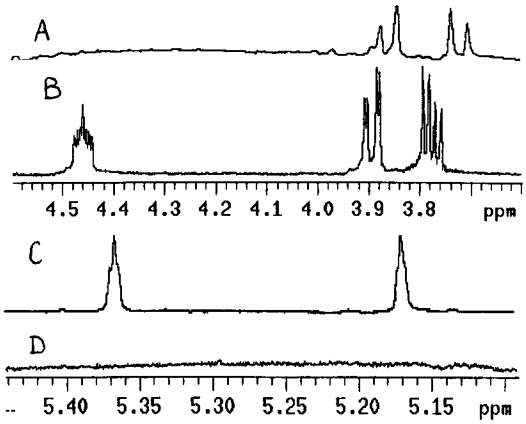

FIGURE 10: ^1H NMR spectra of 2-PGA following treatment with wild type and H159A enolase. Samples contained 20 mM 2-PGA, 25 μM enzyme in 25 mM Tris buffer in D_2O, pD 7.5, and 50 mM KCl. A spectrum was recorded (not shown) for reference, and the reaction was initiated by addition of 1 mM Mg^{2+}. The reaction containing wild-type enolase was quenched after 10 min by addition of 2.5 mM EDTA, and the spectrum was recorded. Reaction with the H159A enolase was incubated for 3 h at room temperature before quenching with 2.5 mM EDTA and acquiring the spectrum. The upfield region of the spectra containing the resonance for the C-2 proton (~4.46 ppm) and the C-3 hydroxymethyl protons (~3.78 and 3.9 ppm) are shown after treatment with wild-type (A) and H159A (B) enolase. The downfield region of the spectra containing the resonances for the vinyl protons of PEP (~5.17 and 5.37 ppm) are shown after treatment by wild-type (C) and H159A (D) enolase. All ^1H spectra were obtained as the average of 128 scans on a Varian VXR 500 Unity Plus spectrometer.

$^1H/^2H$ Exchange at C-2 of 2-PGA and Phosphoglycolate. It has been shown previously (*31*) that the ability of enolase to ionize the C-2 proton of 2-PGA and of phosphoglycolate to form an intermediate in the partial reaction can be assayed as an exchange of the C-2 proton with solvent D_2O. The capacity of H159A to catalyze the $^1H/^2H$ exchange at C-2 of 2-PGA and of phosphoglycolate was examined to assay the first step in the catalytic event.

2-PGA was incubated with enzyme, and the ^1H spectrum was recorded (spectrum not shown). The upfield region of the spectrum contains a multiplet at ~4.46 ppm for the C-2 proton and a resolved multiplet at ~3.78 and 3.90 ppm for the C-3 hydroxymethyl protons of 2-PGA. The vinyl protons of PEP are found at 5.17 and 5.37 ppm, observed from separate samples.

The reaction of 2-PGA with wild-type enolase was initiated by addition of Mg^{2+}. After 10 min, the reaction was quenched with EDTA. The resulting spectrum is shown in Figure 10A,C. In the upfield region of the spectrum, the resonance corresponding to the C-2 proton of 2-PGA is no longer observed. The multiple resonances, corresponding to the hydroxymethyl proton of 2-PGA, show a less complex splitting pattern (Figure 10A) and an upfield shift of about 0.5 ppm, compared to the reference spectrum (not shown). This is due to the exchange of the C-2 proton of 2-PGA with solvent D_2O. In the downfield region of the spectrum, resonances corresponding to the vinyl protons of PEP are

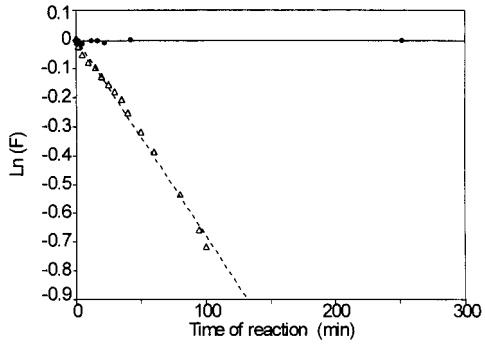

FIGURE 11: Time course of the exchange of the C-2 proton of 2-phosphoglycolate with D_2O. The samples contained 20 mM phosphoglycolate, 25 mM Tris buffer in D_2O, pD 7.5, in the presence of 50 mM KCl, 1 mM Mg^{2+}, and 25 μM wild-type (△) or 25 μM H159A (●) enolase. The area of the ^1H resonance for P-glycolate was measured as a function of time. *F* is the fraction of [2-^1H]-2-phosphoglycolate remaining in the sample.

observed (Figure 10C). Such a spectral change is expected from the catalytically active protein when equilibrium in D_2O is reached. The H159A reaction with 2-PGA in the presence of Mg^{2+} was allowed to proceed for 3 h before being quenched with EDTA. The resulting spectrum is shown in Figure 10B,D. The upfield region of the spectrum is identical to the reference spectrum recorded before the reaction was initiated with Mg^{2+}. No resonances were detected in the downfield region of the spectrum. These results indicate that H159A enolase failed to catalyze the overall dehydration of 2-PGA or proton exchange as the first step of the reaction.

With phosphoglycolate as a substrate, the results of a time course of the exchange reactions catalyzed by wild type and H159A enolase in D_2O are shown in Figure 11. It should be noted that, although the two C-2 protons in phosphoglycolate are magnetically equivalent, enolase will selectively remove only one of these two protons (*32*). The exchange reaction is complete when the height of the [2-^1H]-phosphoglycolate is decreased by 50% compared to the reference spectrum. As illustrated by the data in Figure 11, the exchange reaction catalyzed by the wild type was completed after about 100 min with a rate constant of 0.2×10^{-3}/(min/μM enzyme). The H159A enolase exhibited no activity in this reaction. The results of this experiment show that the H159A enolase does not catalyze the ionization of the C-2 proton of phosphoglycolate.

Chemical Rescue Experiments. There is precedent for chemical rescue of catalytic activity by the addition of exogenous amines as demonstrated when a "critical histidine" of aspartate aminotransferase was removed by mutation (*11*). H159A and H159G (less bulkier side chain) enolase were incubated with (*1*) 50 mM Imidazole at pH 7.5 in the presence of increasing concentrations of Mg^{2+} (1−20 mM) and (*2*) in the presence of CAPS buffer at pH 9.5 and 50 mM NH_4Cl. No enolase activity (<0.01%) was measured under either of these conditions, compared to the activity measured in 50 mM Hepes, pH 7.5.

$^1H/^2H$ exchange at C-2 of 2-PGA and of phosphoglycolate were repeated in the presence of the rescue agents, and no exchange of the C-2 proton with solvent D_2O was observed with either ligand (data not shown). The inability of free imidazole and ammonia to substitute for the imidazole portion of His159 might be due to several reasons; therefore, the results of the chemical rescue experiments are not conclusive.

DISCUSSION

Investigations were made into the role played by His159 in the chemical mechanism of the reaction catalyzed by yeast enolase. These investigations involved an analysis of the overall structural integrity of the H159A protein and formation of the enzyme−metal and enzyme−metal−ligand complexes. The $^1H/^2H$ exchange at C-2 of 2-PGA and phosphoglycolate as a partial reaction in the catalytic mechanism of yeast enolase was analyzed by ^1H NMR.

The sequence of the altered gene shows that the H159A mutant of yeast enolase has been constructed. The mutant protein is expressed and is folded properly as indicated by the near- and far-UV circular dichroism and fluorescence data (Figures 2 and 3). The binding of Mn^{2+} at metal site I, as determined by the EPR measurements, is unaffected by this mutation. The results of the PRR titrations indicate that the substitution of Ala for His at the active site of yeast enolase does not affect the binding of the substrate 2-PGA, the analogue P-glycolate, and the inhibitory ligands F^- and/or P_i to the enzyme−Mn^{2+} complex (Figures 5−7; Table 2). The synergism of F^- and P_i binding is not altered.

The H159A enolase showed reduction in k_{cat} of at least 4 orders of magnitude. The severely depressed activity of the mutant protein indicates that histidine 159 is essential for catalysis. In the routine assay with Mg^{2+} as an activating metal ion and using large excess of the H159A mutant protein compared to that used with wild-type enolase, less than 0.01% activity (compared to the wild type) was detected. This level of activity represents the lower limit of detection for enolase activity. The same levels of activity were obtained after varying the pH of the assay from 5.4 to 10.0 and utilizing Mg^{2+}, Mn^{2+}, or Co^{2+} as activating cations. The activity was too low to measure K_m and K_a values. The lack of catalytic activity was not caused by an observable change in protein structure nor by a loss in substrate or cation binding. Cation and substrate binding to enolase is a more sensitive probe for structure alterations of the protein than are spectroscopic changes. The H159A mutation appears to result in no alterations in the structure of enolase. To gain further insight into the specific role played by His159, the capacity of the mutant protein to catalyze the $^1H/^2H$ exchange at the C-2 of 2-PGA and the substrate analogue, phosphoglycolate, were examined. This reaction is the first step, the removal of the proton at C-2, in the catalytic process (*32*, *33*). The results shown in Figures 10 and 11 clearly indicate that H159A fails to ionize the C-2 proton of either 2-PGA or phosphoglycolate. This deprotonation process is facile with wild-type enolase. These findings are consistent with His159 serving as a potential catalytic base in the enolase reaction.

From the crystal structure by Poyner and Reed (*34*) Lys396 is positioned at the C-3 hydroxymethyl site of 2-PGA and is capable of donating a proton to the leaving hydroxyl group. It has been observed that His159 and Lys396 are located on the opposite sides of the substrate as seen in several crystal structures (*1*−*3*). We suggest that His159−Lys396 is the catalytic acid−base pair in yeast enolase but the roles they play in catalysis are reversed from those previously proposed (*34*) (Figure 12).

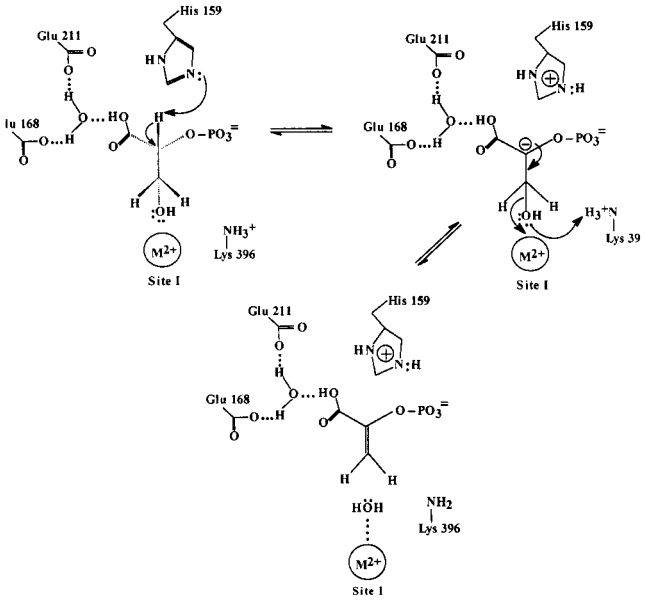

FIGURE 12: Proposed catalytic mechanism of yeast enolase. This mechanism is a modification of that proposed by Duquerroy et al. (*3*) and consistent with results discussed in the text.

In the crystal structure by Duquerroy et al. (*3*) lobster muscle enolase is complexed with Mn^{2+} and phosphoglycolate, the inhibitor, which lacks the hydroxymethyl moiety of the true substrate. Nevertheless the position of this missing group is fully determined by the known stereospecificity for the (*D*)-enantiomer of 2-PGA in the reaction. As elimination occurs anti to the C_2 proton (*5*), the orientation of the hydroxymethyl group is also trans to the proton abstracted from the C-2 position. If the base is His159, the hydroxyl group at C-3 is in position to bind to the metal at site I. If the base is Lys345, the hydroxymethyl group cannot bind the metal. Poyner et al. (*4*) proposed that the metal ion at site I ligates the carboxylate instead of the hydroxyl. This interpretation differs from the structure proposed by Lebioda and Stec (*1*) and by Duquerroy et al. (*3*) from their X-ray diffraction data. In both of those X-ray structures the carboxylate was found not to ligate the metal. Such observation is also consistent with a large body of biochemical evidence including NMR results (*26*), as reviewed by Brewer (*34*, *35*), showing that the metal at site I binds the C-3 hydroxyl group.

The results of the PRR experiments to determine the hydration number of the metal ion at site I in the H159A−Mn−PGA and H159A−Mn−PEP complexes (Figure 9 and Table 3) complement the results of Lebioda and Stec (*1*) and of Duquerroy et al. (*3*). A molecule of 2-PGA bound at the active site of yeast enolase coordinates to the metal ion at site I through the C-3 hydroxyl group (one exchangeable proton). In the case of PEP binding, a water molecule (two exchangeable protons) is positioned between the C-3 and the metal ion at site I.

Vinarov and Nowak (*6*) have shown that optimal enolase catalysis with Mg^{2+} requires a group with a pK_A of about 5.9 to be unprotonated and a group with a pK_A of about 8.5 to be protonated. A histidine residue that is deprotonated and acts as the catalytic base in yeast enolase to abstract the C-2 proton in the initial step of the reaction is consistent with the observed pK_A of 5.9.

Each monomer of apoenzyme has a single binding site for Mg^{2+}. In the presence of substrate, there are up to three cation sites per monomer at neutral pH. Metal binding at site I induces a conformational change in the active site and enables subsequent binding of substrate (*37*). Upon substrate binding, the second metal ion can bind at site II. At higher metal ion concentrations, a third metal ion will bind. This metal ion binding inhibits enzymatic activity (*38*−*40*). It has been shown previously that the third, inhibitory, metal binding site appears to be titrated at a pH value of between 6.5 and 7.0 (*40*) and may be located either at a histidine-containing site, at the phosphoryl group of the substrate, or at both. On the basis of the analysis of several crystal structures of enolase (*1*−*3*) and the results of the pH dependence of the metal inhibition, Vinarov and Nowak (*6*) have proposed that His159 could serve as a metal ligand at the third, inhibitory, metal binding site. This proposal is consistent with the proposed catalytic mechanism of yeast enolase. When Mg^{2+} binds at site III, the metal ion competes with the C-2 proton for the same position on the histidine residue. As a result, the pK_A for the catalytically important histidine is increased. Therefore, at the pH for optimal catalysis (pH = 7.5) and in the presence of excess divalent cation, this histidine is only partially deprotonated, leading to a decrease in k_{cat} but not a total loss in catalytic activity.

The results of the metal binding studies presented in this paper are consistent with this proposal. The H159A mutation has no effect on the Mn^{2+} binding at sites I and II. The binding of Mn^{2+} at the third, inhibitory site is about one-third as strong as the binding of Mn^{2+} to the wild-type enolase complex. The factor of 3 decrease in binding is reasonable for the contribution to binding strength of a single nondominant ligand in a chelate (*41*−*43*).

Toney and Kirsch (*11*) have demonstrated that inactivation of aspartate aminotransferse due to the mutation of the catalytic residue K258 to an alanine can be overcome by the exogenous addition of small molecule amines. Chemical rescue in a study of yeast enolase catalysis was attempted. In the initial experiments, H159A was treated with two rescue agents: imidazole and ammonia. Catalytic activity was measured as was the C-2 proton exchange of 2-PGA and phosphoglycolate in D_2O. Neither imidazole nor ammonia succeeded in reviving the catalytic activity of the mutant protein. It has been shown (*44*) that, for the purpose of chemical rescue experiments, a glycine residue is a better choice than an alanine at the histidine site. H159G enolase was designed and expressed, and the mutant protein was also inactive. This mutant enzyme was treated with imidazole and ammonia. Results, identical to the H159A rescue attempts, were obtained. The inability of free imidazole to substitute for the imidazole portion of His159 might be due to several reasons. One possibility is that free imidazole could not diffuse into the cavity created by the mutations of His159 to alanine or glycine. Ammonia, which occupies a molecular volume almost one-third that of free imidazole, also had no affect on the catalytic activity of H159A or H159G enolase. The results of the chemical rescue experiments are nonconclusive.

Figure 12 summarizes our conclusions concerning the catalytic mechanism of enolase. In this figure, the carboxylate of 2-PGA is protonated by the Glu168−H_2O−Glu211 proton relay system and His159 acts as the base to initiate the

deprotonation of 2-PGA. As His159 removes the α-proton, the negative charge on C_2 becomes delocalized. The charge is distributed over several adjacent atoms, the metal at site I favoring delocalization to the hydroxymethyl oxygen rather than on the aci-carboxylate oxygens of an enolic intermediate. This is consistent with findings by Stubbe and Abeles (*31*) showing that the presence of the hydroxyl group on the substrate facilitates the proton abstraction. In addition to lowering the free energy of carbanion formation, the charge developing on the hydroxyl group should help β-elimination by weakening the C−O bond. In the second step of the reaction, the proton is transferred from the amine of Lys396 to the leaving hydroxyl group. The resulting water molecule enters the coordination sphere of metal ion at site I. This model is consistent with results obtained by Nowak et al. (*26*), Nowak and Maurer (*27*), and the PRR results herein.

In summary, the results presented in this paper have shown that the His159 is a viable candidate for the general base in the enolase reaction. This proposal is consistent with the mechanism of yeast enolase catalysis, metal ion inhibition, and the pH rate profile (*6*).

ACKNOWLEDGMENT

The authors thank Don Schifferl and Dr. Jaroslav Zajicek for help in setting up the NMR experiments and Dr. Michael Buening for helpful discussions.

REFERENCES

1. Lebioda, L., and Stec, B. (1991) *Biochemistry 30*, 2817−2822.
2. Larsen, T. M., Reed, G. H., Wedekind, J. E., and Rayment, I. (1996) *Biochemistry 35*, 4349−4358.
3. Duquerroy, S., Camus, C., and Janin, J. (1995) *Biochemistry 34*, 12513−12523.
4. Poyner, R. R., Reed, G. H., Laughlin, L. T., and Sowa, G. A. (1996) *Biochemistry 35*, 1692−1699.
5. Cohn, M., Pearson, J. E., and Rose, I. A. (1970) *J. Am. Chem. Soc. 92*, 4095−4102.
6. Vinarov D. A., and Nowak, T. (1998) *Biochemistry 37*, 15238−15246.
7. Lebioda, L., Zhang, E., Lewinski, K., and Brewer, J. M. (1993) *Proteins 16*, 219−225.
8. Wedekind, J. E., Reed, G. H., Poyner, R. R., and Rayment, I. (1994) *Biochemistry 33*, 9333−9342.
9. George, A. L., and Borders, C. L. (1979) *Biochim. Biophys. Acta 569*, 63−69.
10. Holland, M. J., Holland, J. P. Thill, G. P., and Jackson, K. A. (1981) *J. Biol. Chem. 256*, 1385−1395.
11. Toney, M. D., and Kirsch, J. F. (1989) *Science 243*, 1485−1488.
12. Lee, M. E., and Nowak, T. (1992) *Biochemistry 31*, 2172−2180.
13. Warburg, O., and Christian, W. (1941) *Biochem. Z. 310*, 384−421.
14. Chin, C. C. Q., Brewer, J. M., and Wold, F. (1981) *J. Biol. Chem. 256*, 1377−1384.
15. Westhead, E. W., and McLain, G. (1964) *J. Biol. Chem. 239*, 2464−2468.
16. Scatchard G. (1949) *Ann. N.Y. Acad. Sci. 51*, 660−672.
17. Winlund, C. C., and Chamberlin, M. J. (1970) *Biochem. Biophys. Res. Commun. 40*, 43−48.
18. Carr, H. Y., and Purcell, E. M. (1954) *Phys. Rev. 94*, 630−638.
19. Hwang, S. H., and Nowak, T. (1989) *Arch. Biochem. Biophys. 269*, 646−663.
20. Bloembergen, N., and Morgan, L. O. (1961) *J. Chem. Phys. 34*, 842−850.
21. Solomon, L. (1955) *Phys. Rev. 99*, 559−565.
22. Solomon, L., and Bloembergen, N. J. (1956) *Chem. Phys. 25*, 261−266.
23. Swift, T. J., and Connick, R. E. (1962) *J. Chem. Phys. 37*, 307−320.
24. Jones, D. H., McMillan, A. J., and Fersht, A. R. (1985) *Biochemistry 24*, 5852−5857.
25. Cohn, M. (1963) *Biochemistry 2*, 623−629.
26. Nowak, T., Mildvan, A. S., and Kenyon, G. L. (1973) *Biochemistry 12*, 1690−1701.
27. Nowak, T., and Maurer, P. J. (1981) *Biochemistry 20*, 6900−6911.
28. Maurer, P. J., and Nowak, T. (1981) *Biochemistry 20*, 6894−6900.
29. Navon, G. (1970) *Chem. Phys. Lett. 7*, 390−394.
30. Meiboom, S., and Gill, D. (1958) *Rev. Sci. Instrum. 29*, 688.
31. Stubbe, J., and Abeles, R. (1980) *Biochemistry 19*, 5505−5512.
32. Dinovo, E. C., and Boyer, P. D. (1971) *J. Biol. Chem. 246*, 4586−4593.
33. Westhead, E. W. (1966) *Methods Enzymol. 9*, 670−679.
34. Poyner, R. R., and Reed, G. H. (1992) *Biochemistry 31*, 7166−7173.
35. Brewer, J. M. (1981) *CRC Crit. Rev. Biochem. 9*, 209−254.
36. Brewer, J. M. (1985) *FEBS Lett. 182*, 8−14.
37. Hanlon, D. P., and Westhead, E. W. (1969) *Biochemistry 8*, 4247−4255.
38. Elliot, J. I., and Brewer, J. M. (1980) *J. Inorg. Biochem. 12*, 323−334.
39. Brewer, J. M., and Ellis, P. D. (1983) *J. Inorg. Biochem. 18*, 71−82.
40. Lee, B. H., and Nowak, T. (1992) *Biochemistry 31*, 2165−2171.
41. Klemba, M., and Regan, L. (1995) *Biochemistry 34*, 10094−10100.
42. Regan, L. (1993) *Annu. Rev. Biophys. Biomol. Struct. 22*, 257−281.
43. Cha, J., Cho, Y., Whitaker, R. D., Karplus, P. A., and Batt, C. A. (1994) *J. Biol. Chem. 269*, 2687−2694.
44. Huang, S., and Tu, S.-C. (1997) *Biochemistry 36*, 14609−14615.

BI990760Q